



Aalborg Universitet

AALBORG UNIVERSITY  
DENMARK

## High-Performance Control of Paralleled Three-Phase Inverters for Residential Microgrid Architectures Based on Online Uninterruptable Power Systems

Zhang, Chi; Guerrero, Josep M.; Vasquez, Juan Carlos; Coelho, Ernane A. A.; Seniger, Carsten

*Published in:*

Proceedings of the 2015 IEEE Applied Power Electronics Conference and Exposition (APEC)

*DOI (link to publication from Publisher):*

[10.1109/APEC.2015.7104815](https://doi.org/10.1109/APEC.2015.7104815)

*Publication date:*

2015

*Document Version*

Early version, also known as pre-print

[Link to publication from Aalborg University](#)

*Citation for published version (APA):*

Zhang, C., Guerrero, J. M., Vasquez, J. C., Coelho, E. A. A., & Seniger, C. (2015). High-Performance Control of Paralleled Three-Phase Inverters for Residential Microgrid Architectures Based on Online Uninterruptable Power Systems. In *Proceedings of the 2015 IEEE Applied Power Electronics Conference and Exposition (APEC)* (pp. 3232 - 3239). IEEE Press. I E E E Applied Power Electronics Conference and Exposition. Conference Proceedings <https://doi.org/10.1109/APEC.2015.7104815>

### General rights

Copyright and moral rights for the publications made accessible in the public portal are retained by the authors and/or other copyright owners and it is a condition of accessing publications that users recognise and abide by the legal requirements associated with these rights.

- Users may download and print one copy of any publication from the public portal for the purpose of private study or research.
- You may not further distribute the material or use it for any profit-making activity or commercial gain
- You may freely distribute the URL identifying the publication in the public portal -

### Take down policy

If you believe that this document breaches copyright please contact us at [vbn@aub.aau.dk](mailto:vbn@aub.aau.dk) providing details, and we will remove access to the work immediately and investigate your claim.

# High-Performance Control of Paralleled Three-Phase Inverters for Residential Microgrid Architectures Based on Online Uninterruptable Power Systems

Chi Zhang\*, Josep M. Guerrero\*, Juan C. Vasquez\*, Ernane A. Coelho\*<sup>#</sup> and Carsten Seniger<sup>†</sup>

Email: {zhc, joz, juq, eac} @et.aau.dk carsten.seniger@leaneco.dk

\*Department of Energy Technology, Aalborg University, Aalborg, Denmark

<sup>#</sup> Universidade Federal de Uberlandia, Brazil

<sup>†</sup> Leaneco A/S, DK-6000 Kolding, Denmark

**Abstract**— In this paper, a control strategy for the parallel operation of three-phase inverters forming an online uninterruptible power system (UPS) is presented. The UPS system consists of a cluster of paralleled inverters with LC filters directly connected to an AC critical bus and an AC/DC forming a DC bus. The proposed control scheme is performed on two layers: (i) a local layer that contains a “reactive power vs phase” in order to synchronize the phase angle of each inverter and a virtual resistance loop that guarantees equal power sharing among inverters; (ii) a central controller that guarantees synchronization with an external real/fictitious utility, and critical bus voltage restoration. Constant transient and steady-state frequency, active, reactive and harmonic power sharing, and global phase-locked loop resynchronization capability are achieved. Detailed system topology and control architecture are presented in this paper. Also a mathematical model was derived in order to analyze critical parameters effect on system stability. An experimental setup was built in order to validate the proposed control approach under several case-study scenarios. Finally, a conclusion is presented.

**Keywords**— Uninterruptible power system, parallel inverters, microgrid, droop control.

## I. INTRODUCTION

With the active development of technologies regarding modern communication systems, advanced medical equipment, advanced living facilities and emergency systems that requires high quality energy are flourishing in everyday life, which require more reliable, efficient electricity supply [1]. A large number of such kind modern loads bring an imposing challenge to the existing electricity supply system. Increasing concerns about the reliability, power quality of the utility leads to growing demand for emergency electricity supply system [2]. Consequently, uninterruptable power systems (UPS) are receiving more and more attention from both engineers and researchers.

On the basis of the International Electrotechnical Commission Standard 62040-3, a UPS system can be divided into three categories, namely offline UPS [3], [4], line interactive UPS [5], [6] and online UPS [7], [8] according to the energy flow direction under normal utility condition. Due to its outstanding capability of suppressing the utility's distortion and interferences, online UPS systems are

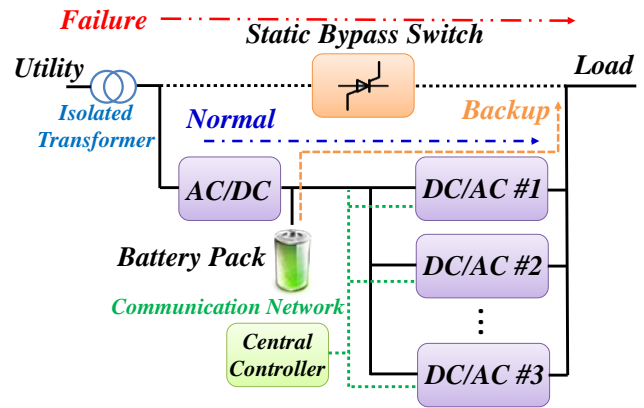


Fig. 1. Proposed Online UPS Structure

proliferating rapidly recently for both high power and voltage application scenarios [7]–[13].

Normally, an online UPS system is composed of AC/DC, DC/AC, a battery pack, a static bypass switch and isolated transformers as shown in Fig. 1. The AC/DC takes the responsibility of regulating DC bus and acts as battery-pack charger at the same time under normal condition (Normal). Otherwise, the online UPS system switches to backup mode and battery pack or diesel generator will regulate DC bus voltage instead of AC/DC (Backup). On the other hand, the static bypass switch transfers the load to the AC input directly in case of power conditioner failure [7] (Failure as shown in Fig. 1).

In order to achieve high reliability, flexibility and power rate, a cluster of DC/AC modules are employed to work together as the DC/AC stage in an online UPS system. As a result, parallel technologies, which are crucial to implement DC/AC parallel operation, are proposed in [14]–[19]. Until now, numbers of parallel solutions, namely centralized control [14], master-slave control [15], [16], averaged load sharing [17], [18], wired distributed control [19] have been proposed. Nevertheless, critical lines between each DC/AC modules are mandatory, which decreases parallel operation's reliability and increases system's complexity. Consequently, a number of wireless droop methods [20], [21] were proposed to avoid critical interaction lines among different DC/AC modules. Local information of each DC/AC, namely active power and

reactive power, is used to regulate DC/AC output voltage amplitude and frequency, which contributes to power sharing among modules. However, their output voltage becomes load dependent. As a result, secondary controllers are designated to compensate voltage deviations and enhance parallel operation performance [22], [23]. Information, such as references, local data of each DC/AC module can be exchanged through communication network since mature DSP technologies have contribute to a smaller communication delay with CAN bus [24].

In this paper, a parallel control approach for online UPS system is proposed. DC/AC is connected to AC critical bus with LC-type filter directly as shown in Fig. 1. Here, only inductor current and capacitor voltage are measured, thus resulting in a cost-effective solution if one current sensor is removed. By calculating reactive power, phase angle is regulated (called reactive power vs phase loop), which aims at achieving reactive power sharing. Consequently, system frequency can be locked at 50Hz all the time in different load condition, which means a much simpler bypass process. At the same time, a virtual impedance loop [21] is inserted into the control loop in order to achieve active power sharing performance considering inductor current. Moreover, a central controller is employed in order to compensate voltage sags and phase drift due to reactive power vs phase loop and the virtual impedance loop. Through communication network (CAN bus), a central controller is used to derive compensated voltage references, which will be used by local controller, and exchange with DC/AC modules.

This paper is organized as follows. Section II discusses the UPS topologies that are being used and presents the proposed control structure. In order to analyze system stability, mathematical model is presented and analyzed in Section IV. Experimental results are presented in Section V to prove the proposed control approach's feasibility. Finally, conclusions are given in Section VI.

## II. PROPOSED CONTROL SCHEME FOR ONLINE UPS SYSTEM

Compared with offline UPS and line-interactive UPS, online UPS, also referred as inverter preferred UPS or double conversion UPS, mainly aims at high power and voltage application due to the full controllability of its output voltage and decoupling capability of the utility and the load under power outage [7], [8]. Based on typical online UPS system, a cluster of improved online UPS systems are proposed during the decades, who are more skilled at regulating active power to achieve unity power factor [9]-[13]. Additional DC/DC [9], [10], high frequency transformer [11], [12] and modular structure are three main issues that are chosen to achieve a cost-effective, volume-effective and more reliable online UPS system [13].

The modular online UPS system employed in this paper, shown in Fig. 1, uses a conventional controlled three-phase AC/DC to regulate a 650V DC bus. The control is achieved in  $dq$  frame, which is illustrated in [25] detailed. Furthermore, the phase information of the utility detected by the AC/DC is also employed as the phase references for DC/AC modules.

### A. Local Controller for DC/AC Module

Conventional double loop control (Fig. 2) in  $\alpha\beta$  is considered in the paper. PR controller with harmonic compensation capability [26], [27] referring to (1) and (2), is used,

$$G_v(s) = k_{pv} + \frac{k_{rv}s}{s^2 + \omega_o^2} + \sum_{h=5,7,11} \frac{k_{hrv}s}{s^2 + (\omega_o h)^2} \quad (1)$$

$$G_c(s) = k_{pc} + \frac{k_{rc}s}{s^2 + \omega_o^2} + \sum_{h=5,7,11} \frac{k_{hrc}s}{s^2 + (\omega_o h)^2} \quad (2)$$

being  $k_{pv}$ ,  $k_{rv}$ ,  $\omega_o$ ,  $k_{hrv}$ ,  $h$ ,  $k_{pc}$ ,  $k_{rc}$  and  $k_{hrc}$  as voltage proportional term, fundamental frequency voltage resonant term, fundamental frequency, the  $h^{th}$  harmonic voltage compensation term, harmonic order, current proportional term, fundamental frequency current resonant term and the  $h^{th}$  harmonic current compensation term respectively. Hereby, only  $5^{th}$ ,  $7^{th}$  have been taken into consideration.

Furthermore, virtual impedance and “reactive power vs phase” loop, referring to (3) and (4), are embedded into control loops to achieve parallel operation and active, reactive power sharing (shown in Fig. 3).

$$V_{nk} = V_{nkref} - R_{vir} i_{nLk} \quad (3)$$

$$\delta_n = \delta_{nkref} + k_{ph} Q_{nk} \quad (4)$$

Here  $n$  is the number of DC/AC module (1, 2, 3...N),  $k$  is the phase order ( $a$ ,  $b$ ,  $c$ ),  $V_{nkref}$  is the nominal voltage reference,  $R_{vir}$  is the virtual resistor,  $\delta_{nkref}$  is the nominal phase reference,  $k_{ph}$  is the phase regulating coefficients and  $Q_{nk}$  is the reactive power of each phase of each DC/AC module.

Each phase voltage references are calculated and modified respectively, referring to (5), (6) and (7), making preparations for unbalance load compensation,

$$v_a = (V_{aref} - R i_{La}) \cdot \sin(\delta_g + k_{ph} Q_a) \quad (5)$$

$$v_b = (V_{bref} - R i_{Lb}) \cdot \sin(\delta_g + k_{ph} Q_b) \quad (6)$$

$$v_c = (V_{cref} - R i_{Lc}) \cdot \sin(\delta_g + k_{ph} Q_c) \quad (7)$$

### B. Central Controller for UPS System

Due to virtual impedance, each phase voltage of DC/AC modules will have deviations and drops, compared with nominal output voltage amplitude, in case of unbalanced load condition. As a result, voltages should be restored to the nominal value without causing any voltage oscillation according to International Electrotechnical Commission Standard 62040-3. And according to the analysis in Section I, since the utility phase information is employed as the phase references for all DC/AC modules in the online UPS system, there exists a phase difference between the utility voltage and actual UPS output voltage, which is an undesired condition for an online UPS system. Thus a central controller that includes voltage amplitude and phase restoration loops is implemented. Considering that each phase voltage may be faced with different condition, references are generated and modified respectively.

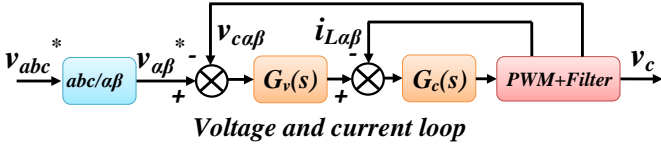


Fig. 2. DC/AC Module inner loop control diagram.

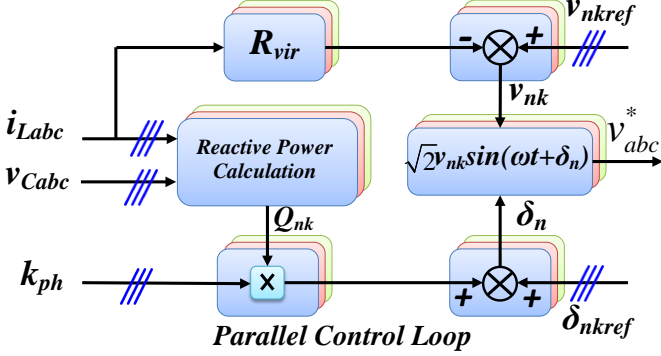


Fig. 3. Virtual impedance and ‘reactive power vs phase’ control diagram.

Each DC/AC sends its own RMS value of capacitor voltage to the central controller through the communication network. Central controller obtains averaged RMS value of each phase voltage respectively (shown in Fig. 4). For instance, average value of all DC/ACs phase *a* RMS voltage is derived,

$$V_{a\_avr} = \frac{1}{n} \sum_{i=1}^n (V_{ia}) \quad (8)$$

where  $V_{ia}$  are phase *a* RMS voltage value of DC/AC #*i*.

Similarly, averaged phase angle information is also calculated in the central controller as follows,

$$\delta_{a\_avr} = \frac{1}{n} \sum_{i=1}^n (\delta_{ia}) \quad (9)$$

where  $\delta_{ia}$  are phase *a* angle of DC/AC #*i*. Through employing a compensation block (Fig. 4), restoration value for voltage amplitude and phase are derived respectively,

$$v_{k\_rec} = (V_{kref\_r} - V_{k\_avr}) \cdot G_{v\_rec}(s) \quad (10)$$

$$\delta_{k\_rec} = (\delta_{kref} - \delta_{a\_avr}) \cdot G_{ph\_rec}(s) \quad (11)$$

being  $v_{k\_rec}$ ,  $k$ ,  $V_{kref\_r}$ ,  $V_{k\_avr}$ ,  $G_{v\_rec}$ ,  $\delta_{k\_rec}$ ,  $\delta_{kref}$ ,  $\delta_{a\_avr}$  and  $G_{ph\_rec}$  as restoration value of voltage amplitude, phase order (*a*, *b*, *c*), RMS voltage reference in central controller, averaged value of each phase RMS voltage value, voltage compensation block transfer function, phase restoration value of voltage phase, phase reference in central controller (utility phase angle), averaged value of phase angle and phase compensation blocks transfer function respectively,

In this scenario, the compensation blocks are implemented by using two typical *PI*s, shown in (12) and (13),

$$G_{v\_rec}(s) = k_{pv\_sec} + \frac{k_{iv\_sec}}{s} \quad (12)$$

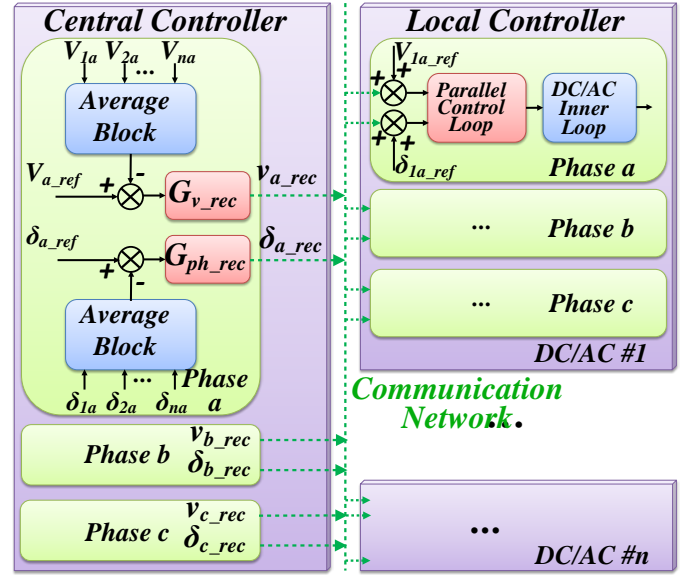


Fig. 4. Overall control diagram for the online UPS system.

$$G_{ph\_rec}(s) = k_{p\theta\_sec} + \frac{k_{i\theta\_sec}}{s} \quad (13)$$

with  $k_{pv\_sec}$  being the voltage proportional term,  $k_{iv\_sec}$  being the voltage integral term,  $k_{p\theta\_sec}$  being the phase proportional term and  $k_{i\theta\_sec}$  being the phase integral term.

### III. STABILITY ANALYSIS

In order to analyze different critical control parameters effect on system performance, detailed mathematical model is derived in this section. Considering that the whole system control scheme is composed of three main parts, namely inner voltage and current loop, power sharing loop (virtual impedance and ‘reactive power vs phase’) and central control (voltage amplitude and phase restoration), system model can be divided into three parts, which are illustrated detailed in the following subsections.

#### A. Analysis of Inner Voltage and Current Loop

According to Fig. 2, transfer function of the inner loop is derived as (15) by giving a PWM delay  $G_{PWM}$ , referring to (14),

$$G_{PWM}(s) = \frac{1}{1.5T_s s + 1} \quad (14)$$

where  $T_s$  is the PWM period. So by combining (1), (2), (9) and (14), transfer function from reference voltage to output capacitor voltage is derived,

$$G(s) = \frac{d}{as^2 + bs + c} \quad (15)$$

with  $a = LR_{Load}C$ ,  $b = L + G_{current}G_{PWM}R_{Load}C$ ,

$c = R_{Load} + G_{current}G_{PWM} + G_{voltage}G_{current}G_{PWM}R_{Load}$ ,

where  $L$ ,  $C$  and  $R_{Load}$  are filter inductance, filter capacitance and load respectively. By combining (1), (2), (14) and (15),

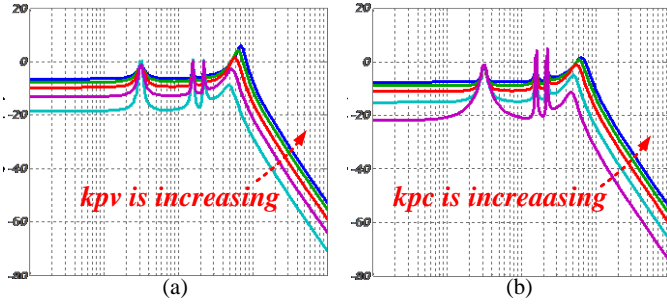


Fig. 5. Bode diagram of inner loop. (a) Bode diagram with variable  $k_{pv}$ . (b) Bode diagram with variable  $k_{pc}$ .

the influence of control parameters on the fundamental frequency and 5<sup>th</sup>, 7<sup>th</sup> harmonic frequency is analyzed through plotting Bode diagram of the system is presented in Fig. 5. It can be observed that 0dB gain has been achieved at both 50Hz and harmonic frequency, which is analyzed detailed in [28].

### B. Virtual Impedance and Reactive Power-to-Phase Droop

Output voltage amplitude is decreased proportionally to the inductor current if the virtual impedance value is fixed. According to the IEC 62040-3, voltage variation should be limited to around 10% due to different load condition. So virtual impedance value can be chosen as,

$$\left| \frac{i_L R_{vir}}{V_{max}} \right| \leq 0.1 \quad (16)$$

being  $i_L$ ,  $V_{max}$  as the inductor current under full load condition and nominal output voltage amplitude respectively. As for the “reactive power vs phase” loop, it is analyzed together with the phase restoration loop since it is tightly related with output voltage’s phase angle.

### C. Central Controller

According to the aforementioned analysis, since the central controller corresponds with UPS output voltage amplitude and phase, its mathematical model can be divided into two parts. In Fig. 6, voltage and phase restoration control is presented with  $G_{delay}$  being the delay function caused by communication network. Because each DC/AC module output capacitors are connected to the same AC critical bus,  $v_{avr}$  is able to be treated equal to  $v_c$ , referring to (8). On the other hand,  $v_c$  is tightly controlled by local control loops from the perspective of communication frequency since dynamics of local controller is much faster than communication. As a consequence,  $v_c$  is able to be treated as the modified voltage reference  $v$ . So the model for voltage restoration is able to be simplified as shown in Fig. 6 (amplitude restoration). By given  $G_{delay}$  a similar pattern as  $G_{PWM}$  but with a bigger  $T_c$ , the mathematical model can be derived,

$$v = \frac{G_{v\_rec} G_{delay} v_{ref\_r} + v_{ref} - R_{vir} i_L}{1 + G_{v\_rec} G_{delay}} \quad (17)$$

Considering the dynamic performance of the system, the closed loop function is expressed as follows,

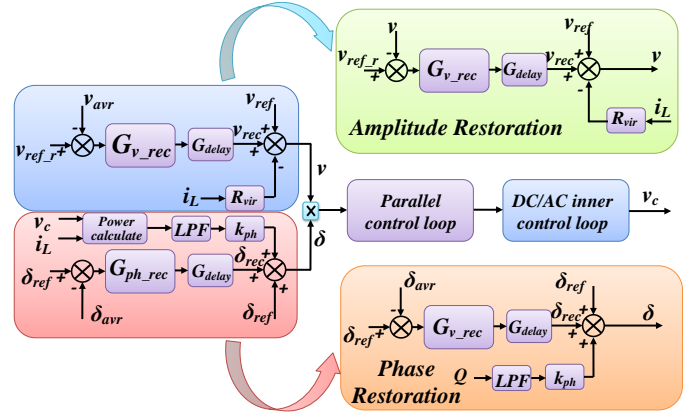


Fig. 6. Control loops for voltage restoration and phase restoration.

$$G_v(s) = -\frac{1.5R_{vir}T_s s^2 + s}{1.5T_s s^2 + (1 + k_p)s + k_i} \quad (18)$$

Fig. 7 shows the  $pz$  map of voltage restoration control block. While  $k_{pv\_sec}$  is moving from 0 to 2, one dominating pole moves obviously towards origin point while the second one tends to move inconspicuously towards boundary of stable area, as shown in Fig. 7(a). Also, it can be observed that  $k_{iv\_sec}$  has indistinctive effect on the dominating poles’ movements. Both two dominating poles almost stay in the same position with changing  $k_{iv\_sec}$ . So mainly,  $k_{pv\_sec}$  determines system dominating poles’ position, which indicates crucial impacts on system performance.

Similarly, by considering that the inner double loop works perfectly from the perspective of communication frequency, a simplified control diagram for phase restoration is derived as shown in Fig. 6 (phase restoration), from which a mathematical model is able to be derived,

$$\delta = \frac{G_{ph\_rec} G_{delay} \delta_{ref\_r} + \delta_{ref} + G_{LPF} k_{ph} Q}{1 + G_{ph\_rec} G_{delay}} \quad (19)$$

Consequently, the dynamic system mathematical model is expressed as follows,

$$\delta = \frac{G_{LPF} k_{ph}}{1 + G_{ph\_rec} G_{delay}} Q \quad (20)$$

$$G_{LPF} = \frac{\omega_c}{s + \omega_c} \quad (21)$$

$$\frac{\delta}{Q} = \frac{as^2 + bs}{cs^3 + ds^2 + es + f} \quad (22)$$

$$G_{delay}(s) = \frac{1}{T_c s + 1} \quad (23)$$

with the following parameters:

$$a = 1.5T_c \omega_c k_{ph}, \quad b = \omega_c k_{ph}, \quad c = 1.5T_c$$

$$d = 1.5T_c \omega_c + k_p + 1, \quad e = \omega_c + k_i + k_p \omega_c, \quad f = k_i \omega_c,$$



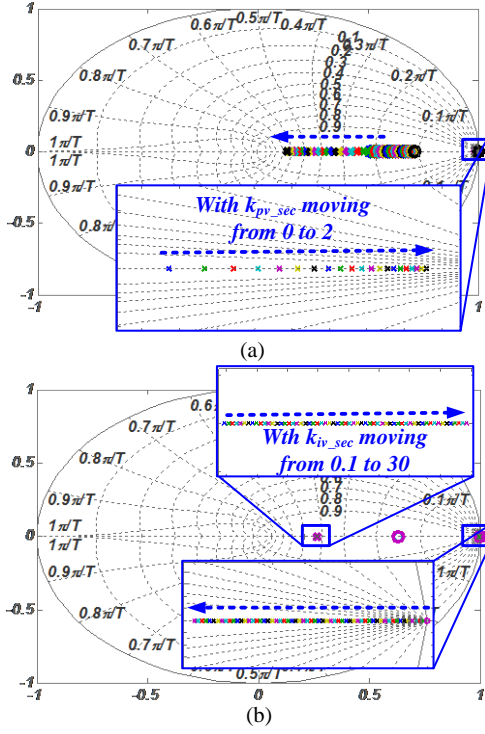


Fig. 7. PZ map of voltage amplitude restoration. (a)  $pz$  map with variable  $k_{pv\_sec}$ . (b)  $pz$  map with variable  $k_{pv\_sec}$ .

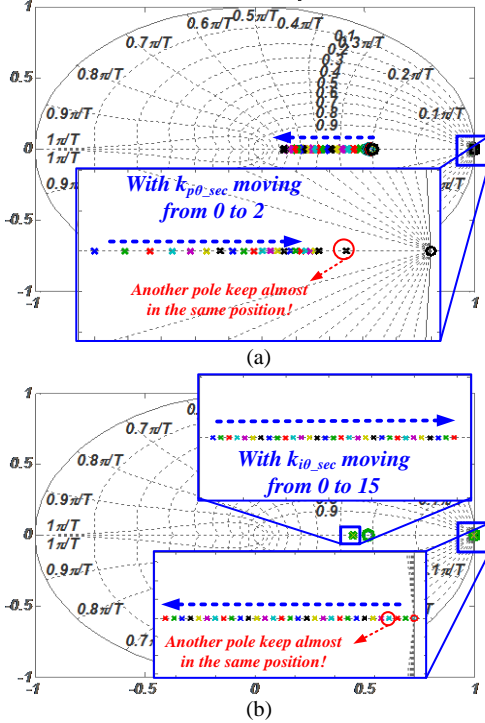


Fig. 8. PZ map for phase restoration. (a)  $pz$  map with variable  $k_{p0\_sec}$ . (b)  $pz$  map with variable  $k_{i0\_sec}$ .

where  $\omega_c$  and  $T_c$  are cut off frequency of power calculation low pass filter and communication delay time respectively. The phase regulation coefficient  $k_{ph}$  is on the numerator, which indicates that it has no effects on system dominating poles distribution. Under different control parameters for phase restoration,  $pz$  map in  $Z$  domain is presented in Fig. 8. It can

be observed that a similar poles and zeros movements performance is obtained, which meaning that proportional term of phase restoration dominates system stability performance.

#### IV. EXPERIMENTAL RESULTS

In order to validate the feasibility of the proposed control approach, an online UPS system shown in Fig. 1 was built in the intelligent microgrid laboratory [29], including four Danfoss converters, shown in Fig. 9. Three of them were working as DC/AC, while the other one was operating as AC/DC converter. The control algorithm was established in MATLAB/SIMULINK and compiled into a dSPACE 1006 platform for real-time control of the experimental setup. A list of critical parameters that have significant effect on the system performance is presented in Table I. Experiments, including both steady and transient operation, were carried out to prove the proposed approach feasibility.

TABLE I. PARAMETERS OF EXPERIMENTAL SETUP

Symbol	Parameter	Values
Converters		
$f_{sw}$	Switch frequency	10kHz
$L$	Filter inductance of DC/AC module	1.8mH
$C$	Capacitor of DC/AC module	27uF
Inverters Control Parameters		
$k_{pv}$	Proportional voltage term	0.55
$k_{rv}$	Resonant voltage term	70
$k_{5rv}, k_{7rv}$	5 <sup>th</sup> , 7 <sup>th</sup> resonant voltage term	100,100
$k_{pc}$	Proportional current term	1.2
$k_{rc}$	Resonant current term	150
$k_{5rc}, k_{7rc}$	5 <sup>th</sup> , 7 <sup>th</sup> , resonant current term	30,30
$V_{ref}$	Reference voltage	230V (RMS)
Secondary Control		
$k_{pv\_sec}$	Proportional voltage term	1
$k_{iv\_sec}$	Integral voltage term	20.5
$k_{p0\_sec}$	Proportional phase term	0.2
$k_{i0\_sec}$	Integral phase term	9

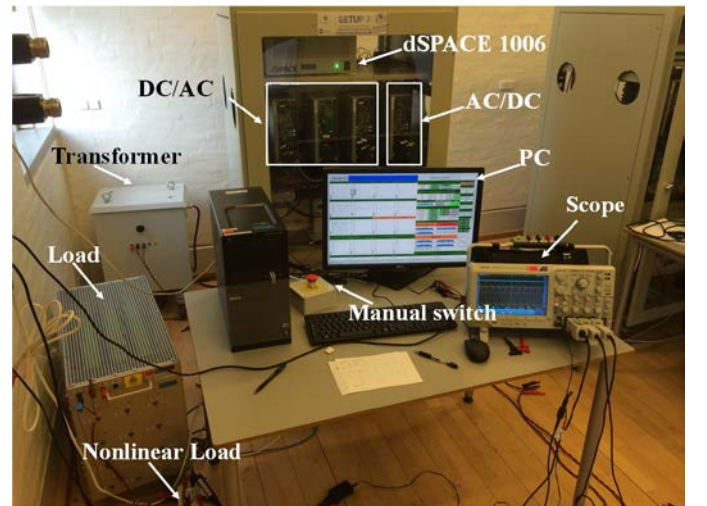


Fig. 9. Experimental setup.

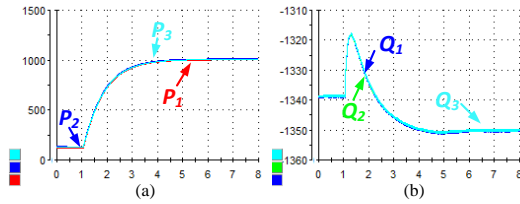


Fig. 10. Active power and reactive power of 3 DC/AC modules. (a) Three DC/ACs' active power. (b) Three DC/ACs' reactive power.

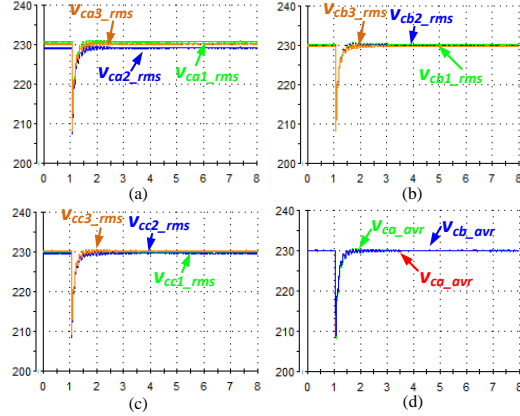


Fig. 11. RMS value of voltage (Three DC/ACs and AC critical bus). (a) Phase a's voltage RMS value. (b) Phase b's voltage RMS value. (c) Phase c's voltage RMS value. (d) AC critical bus' voltage RMS value.

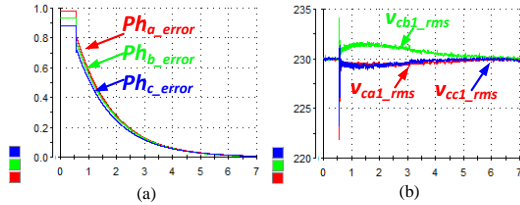


Fig. 12. Phase restoration performance. (a) Phase errors. (b) Voltage value.

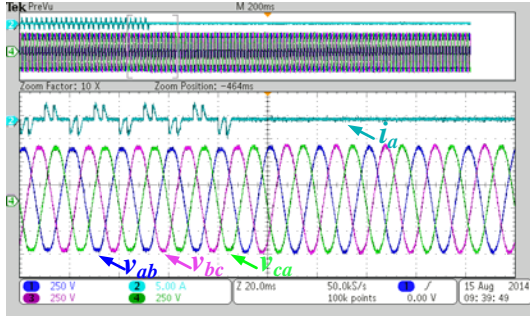


Fig. 13. UPS output voltage and current under nonlinear load condition. (a) Output voltage and phase a's current. (b) Details in case of nonlinear load disconnection.

#### A. Power Sharing Performance

Load step was carried out at around 1s. Accurate power sharing performance under dynamic and steady state was presented in Fig. 10. Due to the low pass filter for power calculation block, power changing process was slowed. Also there is a small reactive power oscillation during the transient process.

#### B. Voltage Restoration Performance

Fig. 11 presents the voltage amplitude restoration performance due to the load step transition. It can be observed

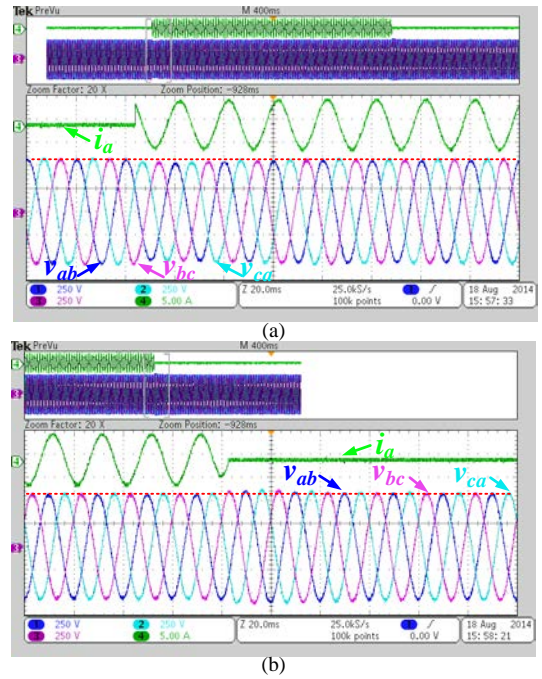


Fig. 14. UPS line to line voltage (phase a to b) and phase a current.

that a 20V RMS voltage sag (around 8.6%), compared to nominal output value, was guaranteed. And this is acceptable according to the International Electrotechnical Commission Standard 62040-3. In Fig. 12, phase restoration performance is presented. Errors between the utility voltage and UPS output (around  $0.9 \times 360^\circ / 2 \times \pi = 51.56^\circ$ ), was reduced to zero once starting the phase restoration control at 0.5s (Fig. 12(a)). However, some impacts had occurred on voltage amplitude as shown in Fig. 12(b). A voltage overshoot (around 4V RMS value) occurred. Because of voltage amplitude restoration control, the amplitude was forced to be back to nominal value after a few cycles.

#### C. UPS Output Terminal Test

Considering the UPS as a whole system, both steady and dynamic performance of the system should be tested at AC critical bus of the UPS system to validate UPS system performance. Nonlinear load, a diode rectifier circuit, was connected with AC critical bus. UPS line-to-line voltage and each phase current were observed through the scope. In Fig. 13, it can be seen that small voltage distortion had occurred when the UPS system was connected with nonlinear load. Also good dynamic performance was presented when the nonlinear load was disconnected. Fig. 14 shows the UPS system performance under linear load condition. It takes around 80ms for the UPS to recover output voltage to nominal value when the load is turned on suddenly. Once shutting down the load, 60ms is required.

#### D. Unbalanced Load Test

Unbalanced load step was also tested in the experimental setup. The load was connected between phases a and b, while phase c was disconnected. The result is shown in Fig. 15. With different load current, AC critical bus voltage is tightly controlled to the nominal output voltage.



### E. Synchronizing Process with the Utility

Synchronization process for the whole UPS system was also tested since online UPS system is required to be kept in phase with the utility voltage at any time. In the experiment, the initial phase error was set to be  $\pi$  by giving a phase delay when the setup is started. In Fig. 16, the total process is illustrated detailed. Four scenarios are chosen to present the synchronizing performance. After starting the phase restoration control, phase error was reduced gradually without bringing any obvious voltage overshoot or sags during the dynamic process.

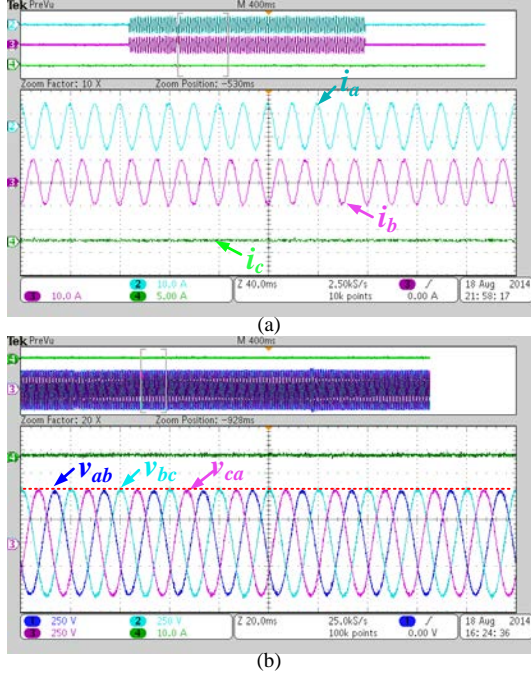


Fig. 15. Voltage and current of steady state in unbalanced load condition. (a) Three phases' current. (b) Output voltage.

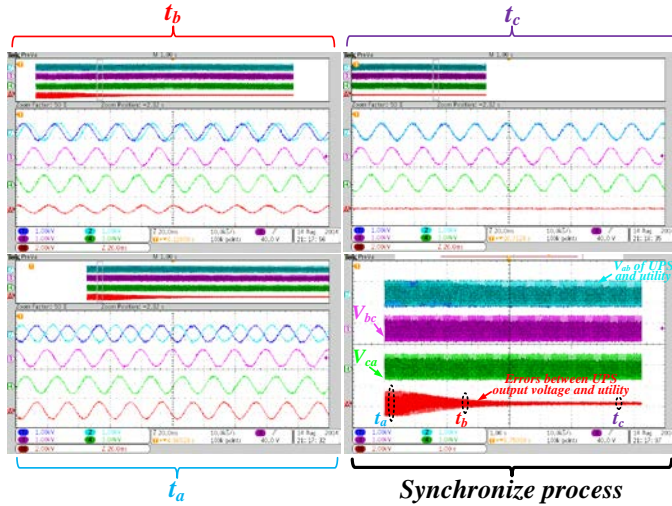


Fig. 16. Synchronizing process between  $v_{ab\_utility}$  and  $v_{ab\_UPS}$ .

### V. CONCLUSION

In this paper, a control strategy intended for an online UPS system was developed under a modular online UPS structure. Active and reactive power sharing performance is validated through experiments results in both steady and dynamic process. Moreover, constant system frequency is performed and global phase lock capability is achieved by combining the proposed local control and central control. The UPS output voltage is kept tightly synchronized with the utility voltage, which means a simple bypass control. The mathematical model of the system is developed and analyzed hierarchically in this paper to analyzed critical parameters impacts. Tests for different load condition had been carried out to prove the feasibility of the proposed control approach. Experimental results are presented to support the proposed control approach's performance.

### REFERENCES

- [1] R.Strzelecki and G. Benysek, *Power Electronics in Smart Electrical Energy Networks*. London, U.K.:Springer. 2008.
- [2] D. Wang, F.Zheng Peng, "Smart Gateway Grid: A DG-Based Residential Electric Power Supply System," *Smart Grid, IEEE Transactions on*, vol.3, no.4, pp.2232,2239, Dec. 2012.
- [3] S. Karve, "Three of a kind [UPS topologies, IEC standard]," *IEE Review*, vol.46, no.2, pp.27,31, Mar 2000.
- [4] S. Martinez, M. Castro, R. Antoranz, F. Aldana, "Off-line uninterruptible power supply with zero transfer time using integrated magnetics," *Industrial Electronics, IEEE Transactions on*, vol.36, no.3, pp.441,445, Aug 1989.
- [5] H. Kim, T. Yu, S. Choi, "Indirect Current Control Algorithm for Utility Interactive Inverters in Distributed Generation Systems," *Power Electronics, IEEE Transactions on*, vol.23, no.3, pp.1342, 1347, May 2008.
- [6] M. de Azpeitia, A. Fernandez, D.G. Lamar, M. Rodriguez, M.M. Hernando, "Simplified Voltage-Sag Filler for Line-Interactive Uninterruptible Power Supplies," *Industrial Electronics, IEEE Transactions on*, vol.55, no.8, pp.3005,3011, Aug. 2008.
- [7] C.C. Yeh; M.D. Manjrekar, "A Reconfigurable Uninterruptible Power Supply System for Multiple Power Quality Applications," *Power Electronics, IEEE Transactions on*, vol.22, no.4, pp.1361,1372, July 2007.
- [8] T.-J. Liang, J.-L. Shyu, "Improved DSP-controlled online UPS system with high real output power," *Electric Power Applications, IEE Proceedings* -, vol.151, no.1, pp.121,127, 9 Jan. 2004.
- [9] J.K. Park; J.M. Kwon; E.H. Kim, B.H. Kwon, "High-Performance Transformerless Online UPS," *Industrial Electronics, IEEE Transactions on*, vol.55, no.8, pp.2943,2953, Aug. 2008.
- [10] E.K. Sato, M. Kinoshita, Y. Yamamoto, T. Amboh, "Redundant High-Density High-Efficiency Double-Conversion Uninterruptible Power System," *Industry Applications, IEEE Transactions on*, vol.46, no.4, pp.1525,1533, July-Aug. 2010.
- [11] R.P. Torrico-Bascope, D.S. Oliveira, C.G.C. Branco, F.L.M. Antunes, "A UPS With 110-V/220-V Input Voltage and High-Frequency Transformer Isolation," *Industrial Electronics, IEEE Transactions on*, vol.55, no.8, pp.2984,2996, Aug. 2008.
- [12] R.P.T. Bascope, C.G.C. Branco, C.M.T. Cruz, E.F. De Oliveira, G.J.M. Sousa, "Proposal of a 5kVA single-phase on-line UPS with high frequency isolation and power factor correction," *Power Electronics Conference, 2009. COBEP '09. Brazilian*, vol., no., pp.886,894, Sept. 27 2009-Oct. 1 2009.
- [13] B. Zhao; Q. Song; W. Liu; Y. Xiao, "Next-Generation Multi-Functional Modular Intelligent UPS System for Smart Grid," *Industrial Electronics, IEEE Transactions on*, vol.60, no.9, pp.3602,3618, Sept. 2013.



- [14] J.M. Guerrero, L.J. Hang, J. Uceda, "Control of Distributed Uninterruptible Power Supply Systems," *Industrial Electronics, IEEE Transactions on*, vol.55, no.8, pp.2845,2859, Aug. 2008.
- [15] J. Holtz, W. Lotzkat, K.-H. Werner, "A high-power multitransistor-inverter uninterruptible power supply system," *Power Electronics, IEEE Transactions on*, vol.3, no.3, pp.278,285, July 1988.
- [16] J.F. Chen, C.L. Chu, "Combination voltage-controlled and current-controlled PWM inverters for UPS parallel operation," *Power Electronics, IEEE Transactions on*, vol.10, no.5, pp.547,558, Sep 1995.
- [17] X. Sun; Y.S. Lee, D. Xu, "Modeling, analysis, and implementation of parallel multi-inverter systems with instantaneous average-current-sharing scheme," *Power Electronics, IEEE Transactions on*, vol.18, no.3, pp.844,856, May 2003.
- [18] Z. Liu, J. Liu, H. Wang, "Output impedance modeling and stability criterion for parallel inverters with average load sharing scheme in AC distributed power system," *Applied Power Electronics Conference and Exposition (APEC), 2012 Twenty-Seventh Annual IEEE*, vol., no., pp.1921,1926, 5-9 Feb. 2012.
- [19] Z. He, Y. Xing, "Distributed Control for UPS Modules in Parallel Operation With RMS Voltage Regulation," *Industrial Electronics, IEEE Transactions on*, vol.55, no.8, pp.2860,2869, Aug. 2008.
- [20] J.M. Guerrero, L. Garcia de Vicuna, J. Matas, M. Castilla, J. Miret, "A wireless controller to enhance dynamic performance of parallel inverters in distributed generation systems," *Power Electronics, IEEE Transactions on*, vol.19, no.5, pp.1205,1213, Sept. 2004.
- [21] W. Yao, M. Chen, J. Matas, J.M. Guerrero, Z. Qian, "Design and Analysis of the Droop Control Method for Parallel Inverters Considering the Impact of the Complex Impedance on the Power Sharing," *Industrial Electronics, IEEE Transactions on*, vol.58, no.2, pp.576,588, Feb. 2011.
- [22] J.M. Guerrero, J.C. Vasquez, J. Matas, L.G. de Vicuña, M. Castilla, "Hierarchical Control of Droop-Controlled AC and DC Microgrids—A General Approach Toward Standardization," *Industrial Electronics, IEEE Transactions on*, vol.58, no.1, pp.158,172, Jan. 2011.
- [23] J.M. Guerrero, M. Chandorkar, T. Lee P.C. Loh "Advanced Control Architectures for Intelligent Microgrids—Part I: Decentralized and Hierarchical Control," *Industrial Electronics, IEEE Transactions on*, vol.60, no.4, pp.1254-1262, April 2013.
- [24] TMS320F2833x, 2823x Enhanced Controller Area Network (eCAN) Reference Guide, TEXAS INSTRUMENTS, January 2009
- [25] R. Teodorescu, M. Liserre, P. Rodríguez, "Grid Converters for Photovoltaic and Wind Power Systems. Grid Converters for Photovoltaic and Wind Power Systems,"
- [26] R. Teodorescu, F. Blaabjerg, M. Liserre, P.C. Loh, "Proportional-resonant controllers and filters for grid-connected voltage-source converters," *Electric Power Applications, IEE Proceedings*, vol.153, no.5, pp.750,762, September 2006.
- [27] A. Timbus, M. Liserre, R. Teodorescu, P. Rodriguez, F. Blaabjerg, "Evaluation of Current Controllers for Distributed Power Generation Systems," *Power Electronics, IEEE Transactions on*, vol.24, no.3, pp.654,664, March 2009.
- [28] J.C. Vasquez, J.M. Guerrero, M. Savaghebi, J. Eloy-Garcia, R. Teodorescu, "Modeling, Analysis, and Design of Stationary-Reference-Frame Droop-Controlled Parallel Three-Phase Voltage Source Inverters," *Industrial Electronics, IEEE Transactions on*, vol.60, no.4, pp.1271,1280, April 2013.
- [29] Aalborg University, Microgrid Research Programme: [www.microgrid.et.aau.dk](http://www.microgrid.et.aau.dk)